Applied Nanoscience (2023) 13:7387–7397
https://doi.org/10.1007/s13204-023-02898-z

ORIGINAL ARTICLE

Metal deposited nanoparticles as "bridge materials" for lead-free solder nanocomposites

Yuriy Plevachuk[1,2] · Peter Švec Sr[2] · Peter Švec[2,3] · Lubomir Orovcik[4] · Otto Bajana[4] · Andriy Yakymovych[5] · Alexander Rud[6]

Received: 24 February 2023 / Accepted: 3 June 2023 / Published online: 7 July 2023
© The Author(s) 2023

Abstract

An influence of carbon nanotubes and carbon nanospheres coated by Au–Pd and Pt on the microstructure of solder/copper joints at room temperature and after aging at sub-zero temperature. The carbon nanosized admixtures were mixed with ternary Sn3.0Ag0.5Cu matrix to prepare a composite solder. The microstructure of the solder joints between the nanocomposite solders and a copper substrate was studied by scanning electron microscopy. It was found that minor (0.05 wt. %) admixtures of both the carbon nanospheres and nanotubes increase the shear strength of the solder joints and reduce the growth rate of the intermetallic Cu_6Sn_5 layer, formed at the interface between solder and copper. This effect may be related to the adsorption of nanoinclusions on the grain surface during the solidification process. Comparative analysis suggests that exposure for 2 months at 253 K does not lead to deterioration of such an important mechanical characteristic of the solder joint as shear strength, indicating the possibility of using these nanocomposite solders in microelectronic equipment even at temperatures below 0 ℃.

Keywords Lead-free solders · Carbon nanoparticles · Solder joint · Microstructure · Shear strength

Abbreviations

LFS	Lead-free solders
SAC305	Sn3.0Ag0.5Cu
CNT	Carbon nanotubes
CNS	Carbon nanospheres
SEM	Scanning electron microscope
TEM	Transmission electron microscope

✉ Andriy Yakymovych
andriy.yakymovych@tuwien.ac.at

Yuriy Plevachuk
yuriy.plevachuk@lnu.edu.ua

[1] Department of Metal Physics, Ivan Franko National University of Lviv, Kyrylo and Mefodiy Str. 8, Lviv 79005, Ukraine

[2] Institute of Physics, Slovak Academy of Sciences, Dubravska Cesta 9, 84511 Bratislava, Slovakia

[3] Centre of Excellence for Advanced Materials Application, Slovak Academy of Sciences, Dubravska Cesta 9, 84511 Bratislava, Slovakia

[4] Institute of Materials and Machine Mechanics, Slovak Academy of Sciences, Dubravska Cesta 9, 84513 Bratislava, Slovakia

[5] Institute of Chemical Technologies and Analytics, TU Wien, Getreidemarkt 9/164, 1060 Vienna, Austria

[6] G.V. Kurdyumov Institute for Metal Physics of NAS of Ukraine, Academician Vernadsky Boulevard36, Kyiv 03142, Ukraine

Introduction

The intensive development of the electronic industry and the related requirements for the miniaturization of solder joints require the improvement of the mechanical properties of lead-free solders (LFS), in particular, the strength and reliability of the joints. The three leading commercial ternary alloys Sn–Ag–Cu (SAC) of near-eutectic or eutectic compositions, known as SAC305, SAC387 and SAC405, are considered the most promising in this regard and are frequently used as materials for lead-free solders in microelectronics (Cheng et al. 2017; Tsao 2011a, b; Gain et al. 2011a, b, c; Haseeb et al. 2012). The demand for such materials with improved stability and reliability is constantly increasing. In this regard, it is important to improve various mechanical and physical properties, such as creep and fatigue resistance, yield strength, thermal resistance, as well as electrical characteristics. Reliability of soldered

joints depends on intermetallic compounds (IMC), which is formed at the boundary of such joints. In the case of a thin IMC layer, the wettability between the solder and the substrate is better, while further growth of the IMC can lead to a weakening of the joints, since intermetallic compounds are known to be brittle. Brittle fractures are caused by different temperature conditions during the processes of thermal cycling and thermal aging, due to different coefficients of thermal expansion between the connecting components and the substrates. However, unlike traditional lead–tin solders, SAC solders generally have higher melting points and higher tin content. Therefore, the formation and further growth of the IMC layer occurs faster in the SAC solder joints, which leads to brittle fractures and a decrease in the service life of the joint due to thermal fatigue (Cheng et al. 2009; Wu et al. 2004; Marques et al. 2013; Li et al. 2012).

To improve the properties listed above, various impurities were added to the SAC solder alloy, which strengthen the basic matrix (see Li et al. 2021 and references therein). It was revealed that nanosized impurities have even more positive effect on increasing the strength of solder joints. This statement was also confirmed by our previous studies, devoted to the influence of nanosized metal Co (Yakymovych et al. 2017a, b), Co-Pd (Yakymovych et al. 2020), Ni (Yakymovych et al. 2017a), Ni–Sn (Yakymovych et al. 2018; Yakymovych et al. 2022) as well as ceramic Al_2O_3, SiO_2, TiO_2, and ZrO_2 (Yakymovych et al. 2016; Aspalter et al. 2020) admixtures on physical properties and the microstructure of Sn–Ag–Cu-based solders. Since shear strength is one of the key mechanical characteristics that ensure the reliability of soldered joints, its improvement is of particular interest and importance. In view of this, the addition of namely nanosized ceramic particles to the solder matrix to form composites is a cost-effective approach to improve the shear strength, as shown by the example of ZrO_2, CeO (Li et al. 2019) or ZnO (Fawzy et al. 2013) admixtures to the SAC matrix.

Among other nanoparticles, carbon nanotubes (CNTs) occupy a prominent place as a reinforcing material. Studies have shown that composite solders with CNTs have better mechanical properties than solders without them. Composite solders exhibit also a lower diffusion coefficient that limits the IMC growth and increases the mechanical strength of solder joints. It was revealed that the dispersion and homogeneous mixing between multi-walled carbon nanotubes and the $Sn_{95.8}Ag_{3.5}Cu_{0.7}$ matrix can be achieved by processes of powder metallurgy (Nai et al. 2008, 2009). Important data about the melting temperatures of hardened alloys were reported in (Kumar et al. 2008).

Besides the filamentous morphology of graphene conducting to CNT, carbon can bond in other different ways to create structures with dissimilar properties. The pairing of pentagonal and heptagonal carbon rings can result in the formation of carbon nanospheres (CNS) (Nieto-Marquez et al. 2011; Rud et al. 2023). This nanostructure attracted recently significant research activity. In its spherical arrangement, the graphite sheets are not closed shells but rather waving flakes that follow the curvature of the sphere, creating many open edges at the surface. Contrary to the chemically inert fullerene, the unclosed graphitic flakes provide reactive dangling bonds that can enhance surface reactions, suggesting CNS as good candidates for catalytic, adsorption and other applications, as well as for the solder alloys strengthening.

One of the problems arising during mixing carbon nanoparticles with the solder is that they are non-wettable by metal melts, so it is very difficult to achieve their homogeneous distribution in the melt, as well as to avoid pushing them out of the molten solder in course of the reflowing. To solve this problem, metallic coatings can be applied to the surface of carbon materials to improve adaptation to the solder matrices before implementation. For example, Ni atoms were deposited on the surface of ceramic reinforcing additions, thus forming core–shell structures (Kumar et al. 2020, 2021). The metal-coated layer formed in this way formed a strong “bridge” that reacted with the lead-free solder matrix to form an intermetallic layer in course of soldering (Han et al. 2012; Chen et al. 2022). A similar positive effect was recently discovered when CNTs were deposited with Au nanosized particles (Plevachuk et al. 2019).

Another important requirement for the LFS application is their reliability in a wide range of operating temperatures, in particular at low temperatures, because for, e.g., application in aerospace conditions, it is important to know the characteristics of the mechanical properties behavior of components during operation in extreme thermodynamic conditions (Wu et al. 2021; Li et al. 2020; Lupinacci et al. 2013; Li et al. 2017). The use of such solders in microelectronic devices at cryogenic temperatures may not be suitable, as Sn-based solders can become brittle due to the allotropic phase transformation of tin, known as “tin pest”.

However, along with the cryogenic temperature range, ensuring the efficient functioning of electronic devices is also important at sub-zero temperatures in terrestrial conditions. Studies of the thermocycling effect at elevated temperatures were carried out (Tan et al. 2015; Tian et al. 2018), but properties behavior of the solder joints in the sub-zero temperature range has not been studied sufficiently. In this work, the influence of multi-walled carbon nanotubes and carbon nanospheres coated with Au–Pd and Pt nanoparticles on the properties of SAC305 solder both at room temperature and after aging for 2 months at 253 K (minus 20 °C), was investigated.

The compositions of the investigated alloys and their designations in the text are given below.

Methods/experimental

Ternary alloy $Sn_{96.5}Ag_3Cu_{0.5}$ (in weight percent) (SAC305) was used as the metal matrix. The SAC305 basic material was employed in a form of a NP505-HR paste from Kester company, which is a zero-halogen solder paste formula for high reliability applications.

Two types of nanosized admixtures, namely, carbon nanotubes (CNTs) and carbon nanospheres (CNSs) were mixed with the basic SAC305 alloy. Carbon spheres were chosen additionally due to the latest data and ideas suggesting that the influence of such admixtures on physical properties of SAC matrix would be also effective. Multi-walled carbon nanotubes with the diameter of about 15–20 nm were synthesized by the method of catalytic pyrolysis (CCVD), using an iron-containing catalyst obtained by coprecipitation of hydroxides of aluminum, magnesium, and ferric iron (Kartel et al. 2016) (Fig. 1).

The electrical discharge methods, based on different principles, namely, the structural phase transformations of carbon that occur as a result of an electrical explosion of graphite, and the low energy electrical discharge action on the molecules of organic liquids, were used for obtaining carbon nanospheres in benzene (CNS1), propane-butane mixture (CNS2) and cyclohexane (CNS3) (Rud et al. 2012) (Fig. 2).

To cover CNT and CNS with Au–Pd and Pt metal vapor precipitates, a high-resolution Gatan ion beam coater (Model 681) was used. The ion beams were generated at ~ 8 keV/300 mA. The system was co-pumped using a liquid nitrogen cold trap placed above the molecular drag pump to further improve the system base pressure.

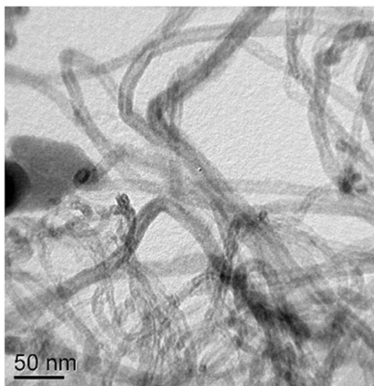

Fig. 1 Carbon nanotubes (TEM)

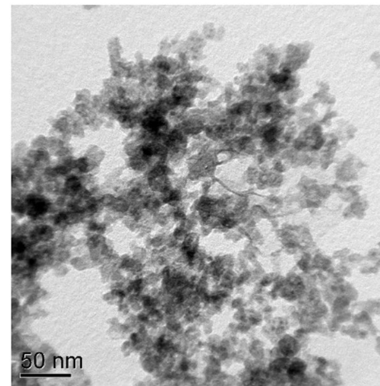

Fig. 2 Carbon nanospheres (TEM)

Since the volume density of CNTs is in the range of 20–40 g/dm^3 that is 3 orders of magnitude less than the density of their walls (approx. 2.2 g/cm^3), nanotubes are extremely light, and therefore, accordingly, have a rather large volume container. Based on analysis of former studies (Plevachuk et al. 2019) the amount of 0.05 wt.% CNTs and CNSs has been added to the SAC305 matrix in present experiments.

For soldered joints, 3 mm thick copper disks with a diameter of 10 and 15 mm were used as substrates. Before applying the nanocomposite solder, we grounded and polished the Cu plates with Al_2O_3 powders, 1 µm and 0.3 µm thick. Samples were cleaned with ethanol and immersed in a 10 vol.% sulfuric acid solution for 2 min to remove the oxide layer arising from the topmost surface. Two copper disks with solder inside were placed in an electric resistance furnace, heated to 523 K and held at this temperature for 300 s. After cooling the solder joints were cleaned of flux residues (Yakymovych et al. 2020). The hardened sample was cut, and its cross-section was carefully prepared for metallographic analysis. The microstructure of the solder joints was investigated by scanning electron microscopy (SEM). JEOL JSM-7600F and JEOL JSM-6610 equipped with an energy dispersive x-ray (EDX) analyzer [Oxford Instruments (OI), X-max 50 mm^2], were used. The COMPO (backscattered electron imaging) and the SEI (secondary electron imaging) modes were used for surface observation. Analysis of the sizes of the intermetallic layers formed between the solder and the copper discs was performed using the Digimizer software. Due to the unevenness of the IMC layers along the interface, an average value of IMC thickness (d) was determined from the following equation:

$$d = S/L, \quad (1)$$

where S is the area of IMC layer obtained from the micrograph and L is the length of the IMC along the interface.

The accuracy of determining the size of the intermetallic layers was ensured by reducing the main sources of Gaussian noise in the digital images using traditional spatial filtering methods to remove noise, such as mean nvolution) filtering, median filtering and Gaussian smoothing, which are available in the Digimizer software.

Morphology of the coated by metals and un-coated CNTs and CNSs were analyzed by transmission electron microscopy (TEM) with a conventional JEOL JEM-2000FX electron microscope operated at 200 kV. The micrographs of the samples have been taken in bright as well as in dark field imaging mode. A typical TEM micrograph of a Au–Pd-coated carbon nanospheres is presented in Fig. 3.

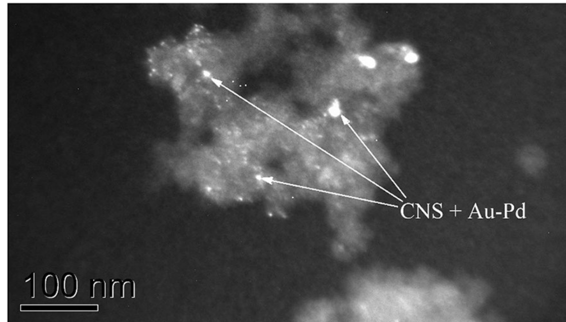

Fig. 3 Carbon nanospheres coated by Au–Pd (TEM)

The shear strength of the solder/substrate joints was determined by a push-off method with a loading rate of 1×10^{-3} m·min^{-1} (Zwick/Roell Z 100).

Results and discussion

Cross-sectional micrographs of the as-solidified joints between SAC305 nanocomposite solders with carbon nanoparticles coated by Au–Pd, Pt and copper substrate are presented in Fig. 4. As can be seen, two intermetallic layers are formed between the bulk solder and the copper substrate, namely, a thinner Cu_3Sn layer in direct contact with the substrate, and a thicker Cu_6Sn_5 layer above it, in contact with the bulk melt. The bulk solder consists of Ag_3Sn and Cu_6Sn_5 particles surrounded by a nearly pure

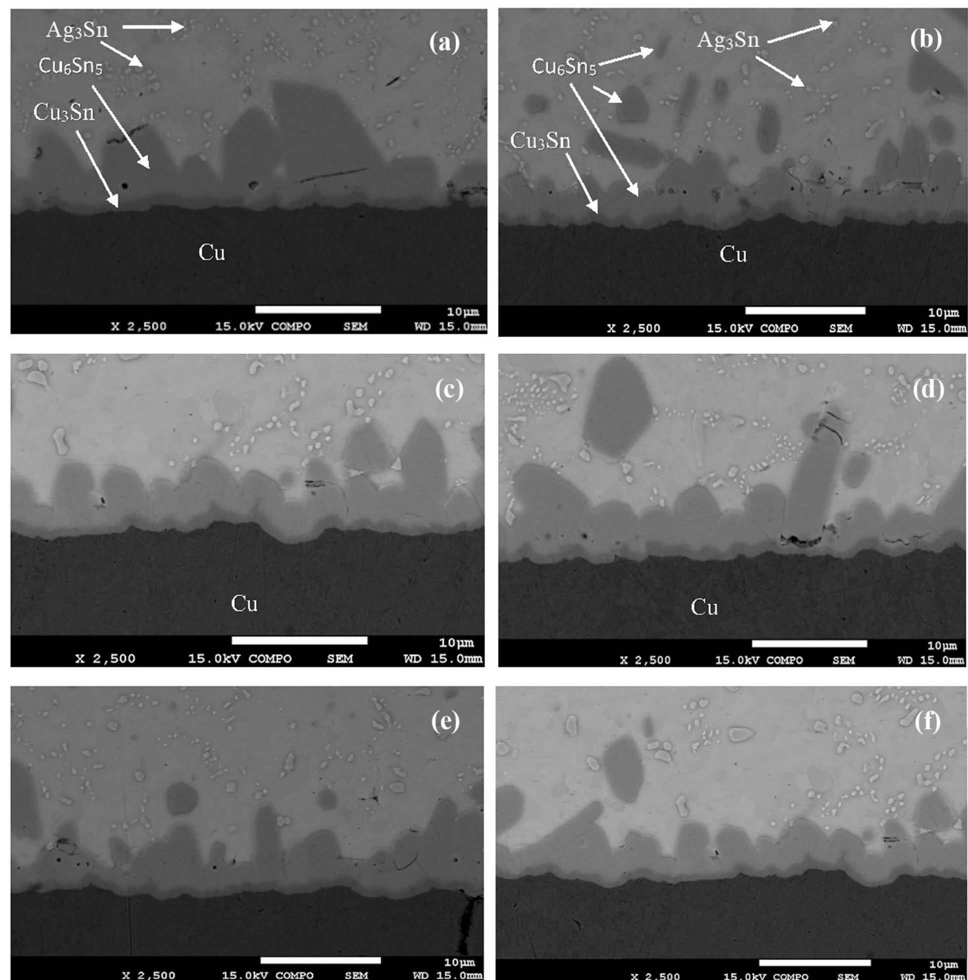

Fig. 4 SEM micrographs of as-solidified SAC305 (**a**) and SAC305 + CNS1 + AuPd (**b**); SAC305 + CNS2 + AuPd (**c**); SAC305 + CNS3 + AuPd (**d**); SAC305 + CNT + AuPd (**e**); 6-SAC305 + CNT + Pt (**f**)

Table 1 The compositions of the investigated alloys and their designations in the text

Alloy composition, wt. %	Designations in the text
Sn3.5Ag0.5Cu	SAC305
Sn3.5Ag0.5Cu-0.05(CNS1 + AuPd)	SAC305 + CNS1 + AuPd
Sn3.5Ag0.5Cu-0.05(CNS2 + AuPd)	SAC305 + CNS2 + AuPd
Sn3.5Ag0.5Cu-0.05(CNS3 + AuPd)	SAC305 + CNS3 + AuPd
Sn3.5Ag0.5Cu-0.05(CNT + AuPd)	SAC305 + CNT + AuPd
Sn3.5Ag0.5Cu-0.05(CNT + Pt)	SAC305 + CNT + Pt

Sn matrix. A small amount of Ag has no influence on the Sn-Cu reaction, and the interfacial phases are similar to those in the pure Sn-Cu couples. In the binary Cu-Sn system, several peritectic reactions occur, resulting in formation of several intermetallic phases. It is known from previous studies that the ε-Cu_3Sn phase as well as the η' -Cu_6Sn_5 phase can exist at the room temperature for the alloy joint enriched with Cu and Sn (see Hwang et al. 2003 and references therein).

The Cu_6Sn_5 intermetallic compound formed typical scallop-type grains at the SAC305/Cu_3Sn interface extending into the solder matrix (Fig. 4a). This intermetallic layer of a scallop-type shape is caused by a dissolution of copper atoms from the substrate into the molten solder until the solder becomes supersaturated with Cu (Laurila et al. 2005). The black dots in the IMC layer are Kirkendall voids formed in the Cu_3Sn/Cu_6Sn_5 and Cu/Cu_3Sn interfaces.

The IMC phases were observed also in the bulk solder (Fig. 4a). Along with rather large Cu_6Sn_5 grains small Ag_3Sn formations also appeared in the bulk matrix but are not visible in the SAC solder/Cu as they are partly adsorbed on the Cu_6Sn_5 surface (Tsao 2011a, b).

Admixtures of the Au–Pd coated CNS to the SAC305 matrix led to some transformation of the solder joint layers where the shape of the scallop-type cusps becomes more rounded, while the thin Cu_3Sn layer that touches the Cu substrate maintains a planar shape (Fig. 4b–d). The same trend was observed in the solder joints between SAC305 containing CNTs coated by Au–Pd or Pt nanoparticles and a copper substrate (Fig. 4e–d). These trends can be explained by similar morphology and the fact that they both consist of sp2 hybridized graphene shells with an interlayer spacing close to that characteristic of graphite. This similarity led to an equally uniform distribution of sputtered metal atoms on the surfaces of both kinds of nanoparticles (See Table 1).

Simultaneously with these processes, the average thickness of the IMC layers at the interface decreased (Fig. 5a). It should be noted that this reduction was experienced in Cu_3Sn as well as in Cu_6Sn_5 layers in all alloys formed by adding the Au–Pd coated CNS1, CNS2, CNS3 and CNTs to the basic SAC305 matrix. The only exception was the solder joint of SAC305 with platinum-coated CNT impurities, where the Cu_6Sn_5 IMC layer exhibited a slight increase (Table 2). The average thickness agrees with the values,

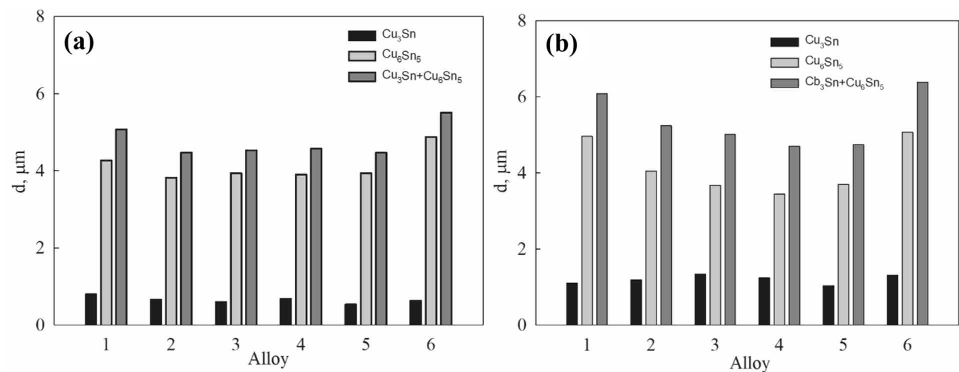

Fig. 5 Average thickness of the interfacial Cu_3Sn and Cu_6Sn_5 IMCs layers formed at the as-reflow Cu/SAC305 + nanoadmixtures/Cu at 293 K (**a**) and after aging for 2 months at 253 K (**b**) 1–SAC305; 2–SAC305 + CNS1 + AuPd; 3–SAC305 + CNS2 + AuPd; 4–SAC305 + CNS3 + AuPd; 5–SAC305 + CNT + AuPd; 6–SAC305 + CNT + Pt

Table 2 Average thickness (d) of the interfacial Cu_3Sn and Cu_6Sn_5 IMCs layers formed at the as-reflow Cu/SAC305 + nanoadmixtures/Cu at 293 K

Alloy	d, µm, Cu_3Sn	d, µm, Cu_6Sn_5	d, µm, $Cu_3Sn + Cu_6Sn_5$
SAC305	0,7981	4,2697	5,0677
SAC305 + CNS1 + AuPd	0,6563	3,8199	4,4763
SAC305 + CNS2 + AuPd	0,5981	3,9334	4,5315
SAC305 + CNS3 + AuPd	0,6757	3,8974	4,5732
SAC305 + CNT + AuPd	0,5351	3,9334	4,4685
SAC305 + CNT + Pt	0,6337	4,8742	5,5079

obtained in our previous studies (Yakymovych et al. 2016; Aspalter et al. 2020). In general, the thickness of the IMC layer can be determined using a simple growth model in which IMC growth is a diffusion-controlled process. Before isothermal aging, the IMC interfacial thickness of the monolithic soldered joint was approximately 10% higher than that of the composite joints. This finding is consistent with statement that the composite solder joints exhibited lower diffusion coefficients, as compared to that of the SAC solder joint (Nai et al. 2009). This signifies that the presence of carbon nanoparticles as reinforcements in the solder joints is effective in retarding the growth of the IMC layer.

Similar phenomena were observed earlier in case of different ceramic admixtures like ZrO_2 (Gain et al. 2011a) or TiO_2, (Leong et al. 2011) and were explained on the basis of the adsorption theory of a surface-active material (Tan et al. 2015; Leong et al. 2011; Wang et al. 2015; Gain et al. 2011b). According to this theory, the admixtures of carbon nanoparticles increase the surfactant content of the solder joint and maximizes the number of adsorbed particles on the surface of intermetallic compounds. But at the same time, an increase in the amount of adsorbed material leads to a decrease in the surface energy of IMCs, which, in turn, results in a slowdown in their growth rate both at the interface and in the volume.

Figure 6 presents the microstructural evolution of the solder joints between the copper substrate and SAC305 matrix armed by CNTs and CNSs nanoadmixtures coated with Au–Pd and Pt, after aging for 2 months at 253 K. As seen from Fig. 6 and Table 3, the morphology of the IMC layers at the solder-substrate interface changed differently in different sample compositions.

The thickness of the Cu_3Sn IMC layer increased almost twice on average, namely, from 0.65 µm to 1.21 µm after 2 months aging at 253 K. As for the Cu_6Sn_5 layer, its thickness did not change so significantly, except for SAC305 without admixtures, where it increased by an average of 16%. As for other solders with impurities, the average

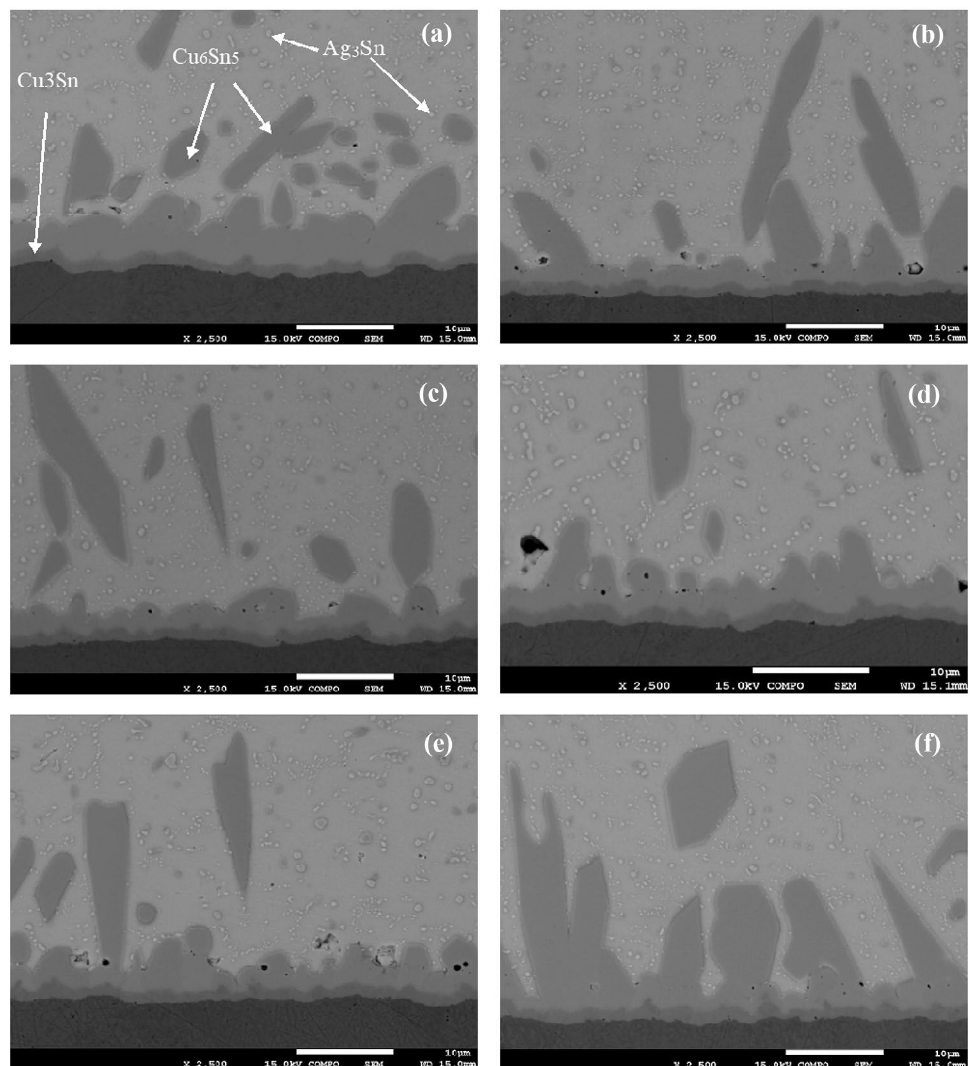

Fig. 6 SEM micrographs of SAC305 (**a**), SAC305 + CNS1 + AuPd (**b**); SAC305 + CNS2 + AuPd (**c**); SAC305 + CNS3 + AuPd (**d**); SAC305 + CNT + AuPd (**e**); 6-SAC305 + CNT + Pt (**f**) after aging for 2 months at 253 K

layer thickness in SAC305 + CNS1 + AuPd increased by only 6% and by 4% in SAC305 + CNT + Pt. In the remaining three samples, this thickness even decreased by 6–12%.

Thus, due to slight changes in the thickness of the Cu_6Sn_5 layer, the total thickness of the intermetallic layers at the junction of the solder with the copper substrate did not increase significantly. The greatest layer extension was observed in the case of SAC305 without admixtures, while the presence of various nanosized impurities slowed down such a growth (Table 4).

Microstructural analysis of the samples also revealed a noticeable change in the shape of the Cu_6Sn_5 formations. As can be seen from Fig. 6, this shape acquires a needle-like structure, and sharp protrusions extending into the metal matrix appear at the solder-substrate interface.

If we consider the microstructure of not only the areas of the joints adjacent to the substrate, but also the general cross-section of the soldered parts, we can see that appearance of the needle-like formations also occurs in the volume of the SAC matrix (Fig. 7).

The detected changes in the microstructure of the solder joints also lead to changes in mechanical properties. That is why, shear strength was measured as one of the main properties of connection reliability. As is seen in Fig. 8a, the addition of three types of carbon nanospheres can noticeably increase the shear strength of the SAC305 solder joints, particularly in the case of CNS3 + AuPd. The admixtures of coated carbon nanotubes also increased the shear strength of the joint.

Tensile results after exposure to low temperature (Fig. 8) showed changes in the level of strength in all tested samples. The data obtained are in agreement with findings revealed by Nai, that admixtures of carbon nanotubes to the solder matrix results in increase of the ultimate shear stress and

Table 3 Average thickness (d) of the interfacial Cu_3Sn and Cu_6Sn_5 IMCs layers formed at the as-reflow Cu/SAC305 + nanoadmixtures/Cu aged for 2 months at 253 K

Alloy	d, μm, Cu_3Sn	d, μm, Cu_6Sn_5	d, μm, $Cu_3Sn + Cu_6Sn_5$
SAC305	1,1118	4,9633	6,0750
SAC305 + CNS1 + AuPd	1,1916	4,0512	5,2429
SAC305 + CNS2 + AuPd	1,3384	3,6719	5,0104
SAC305 + CNS3 + AuPd	1,2491	3,4481	4,6972
SAC305 + CNT + AuPd	1,0362	3,7024	4,7386
SAC305 + CNT + Pt	1,3185	5,0669	6,3854

Table 4 Percentage change in average thickness (Δd) of the interfacial Cu_3Sn and Cu_6Sn_5 IMCs layers formed at the as-reflow Cu/SAC305 + nanoadmixtures/Cu after aging for 2 months at 253 K

Alloy	Δd %, Cu_3Sn	Δd %, Cu_6Sn_5	Δd %, $Cu_3Sn + Cu_6Sn_5$
SAC305	39	16	20
SAC305 + CNS1 + AuPd	82	6	17
SAC305 + CNS2 + AuPd	124	– 7	11
SAC305 + CNS3 + AuPd	85	– 12	3
SAC305 + CNT + AuPd	94	-6	6
SAC305 + CNT + Pt	108	4	16

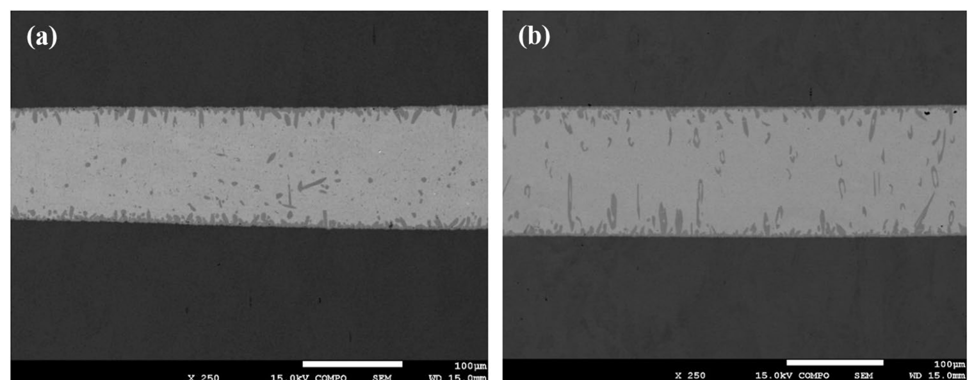

Fig. 7 Microstructure of the Cu/SAC305/Cu soldered cross-section before (**a**) and after aging for 2 months at 253 K (**b**)

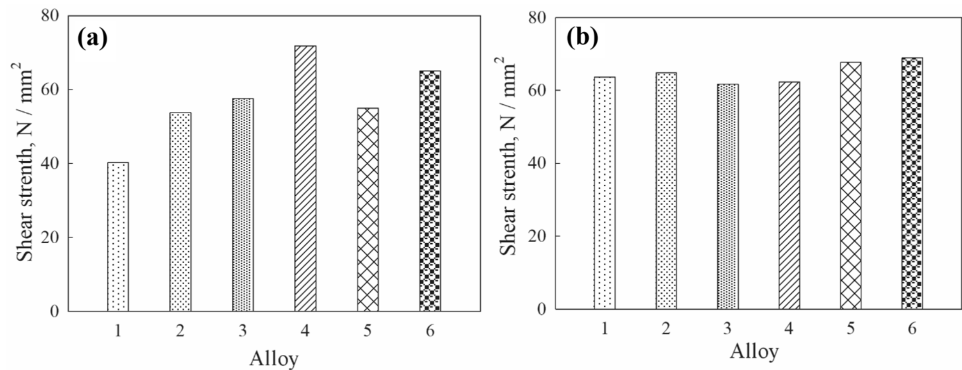

Fig. 8 The shear strength of the nanocomposite SAC305 solder joints at 293 K (**a**) and after aging at 253 K (**b**): 1–SAC305, 2–SAC305 + CNS1 + AuPd; 3–SAC305 + CNS2 + AuPd; 4–C305 + CNS3 + AuPd; 5–SAC305 + CNT + AuPd; 6–SAC305 + CNT + Pt

yield stress of the composite solder joints comparing with the unreinforced solder joint (Nai et al. 2008).

It is well known that chemical reactions between the liquid solder and the solid substrate and subsequent diffusion processes in the solid state result in the IMCs growth. The presence of the IMCs between solders and conductor metals is an indication of good metallurgical bonding. A thin, continuous and uniform IMC layer is an essential requirement for good bonding, which increases the shear strength of a solder joint. Up to a certain thickness, such an intermetallic layer can provide a long-term reliable connection of the solder to the substrate, but its excessive growth will deteriorate the joint. However, due to their inherent brittle nature and the tendency to generate structural defects, too thick IMC layer at the solder/substrate interface may degrade the reliability of the solder joints (Frear et al. 1994). Thus, knowledge of the solder/substrate interactions and phase evolution in the solder interconnections is important for the understanding of the reliability of the solder interconnections from the metallurgical viewpoint and for the optimization of the soldering process.

According to the model proposed in (Wu et al. 1993), there are two limiting conditions for intermetallic formation and growth in the solder/copper substrate system. The first is when diffusion through the growing intermetallic layer is the rate-limiting factor (diffusion-controlled growth). The second is when an interfacial reaction is the rate-limiting step (reaction-controlled growth). It was assumed that the intermetallic formation is a thermally activated process dependent on Sn diffusion.

The formation of the intermetallics probably takes place via the following way. Initially after soldering, thin layers of both Cu_6Sn and Cu_3Sn are formed at the interface. The η-phase, Cu_6Sn_5, forms adjacent to the solder and the ε-phase, Cu_3Sn, forms adjacent to the Cu substrate. Sn diffuses though the Cu_6Sn_5 to the η/ε interface and reacts there with the Cu_3Sn to form Cu_6Sn_5. Sn also diffuses through the Cu_3Sn phase to the Cu_3Sn/Cu interface and reacts there with Cu causing the Cu_3Sn layer to grow in thickness as well. The impurities in composite solders strongly affect the diffusion behavior of Sn and affect the formation of intermetallics at the solder/copper substrate interface, but in different ways. It was established that during annealing of different durations at different elevated temperatures, various admixtures can both increase or decrease the thickness of each of the Cu_3Sn and Cu_6Sn_5 layers, affecting the activation energies of their formation. At the same time, similar studies were not conducted at low sub-zero temperatures. The main result of our research is the conclusion that metal deposited CNTs and CNSs admixtures can slow down the growth of the total amount of intermetallics compared to pure SAC solder. However, the dynamics of the morphology of individual intermetallics requires further research.

However, it should be remembered that adding too many impurities can worsen the mechanical properties of soldered joints. For example, it was reported that the tensile properties improvement for the composites with 0.04 wt.% and 0.07 wt.% of carbon nanotube addition were less significant comparing with 0.01 wt.%. This can be due to the higher level of microporosity found at higher amount of CNTs. The micropores act as centers of stress concentration, which contributed to the formation of microcracks and eventually led to the failure of the material. Besides, the ductility of the composites may decrease with increasing mass percentage of CNTs, as this will occur where the CNTs will be in contact with each other and not with the solder particles. This will result in the formation of small clusters, which will prevent effective bonding between carbon nanotubes and solder particles. Thus, small cracks can appear, which act as nucleation centers of plastic instability, leading to the failure of the material with lower values of plasticity. We assume that the same behavior is possible in the case of carbon nanospheres, which addition to solder matrix has practically not been investigated before. It is possible that the properties of CNSs obtained by different methods are slightly different, and therefore their optimal proportions in the solder should also be different, which concerns, in particular, the shear strength reduction in case of the SAC305 + CNS3 + AuPd alloy.

Finally, it should be noted that the shear strength of soldered joints, like some other mechanical properties, may depend not only on the intermetallic layers formed at the solder/substrate interface, but also on the amount, size and morphology of the intermetallics formed in the solder bulk. At this point, further studies are required.

Conclusions

As a result of prolonged exposure at a low temperature of 253 K, the thickness of the intermetallic layers formed in copper pairs soldered with SAC305 nanocomposite solders containing carbon nanoparticles coated by Au–Pd and Pt increases more slowly than in the case of solders without impurities. The addition of coated carbon nanospheres and nanotubes increased the shear strength of the joints.

There is a noticeable change in the shape of the Cu_6Sn_5 intermetallic areas, which acquire a needle-like structure. Sharp protrusions directed towards the middle of the metal matrix appear at the solder-substrate interface. Needle-like formations are also formed in the volume of the SAC matrix, mainly in the direction perpendicular to the copper substrates.

Thus, the use of the nanocomposite SAC305 solders in electronic devices operating at temperatures as low as –20 ℃ degrees is possible at least up to 2 months, but it should be taken into account that further growth of intermetallic layers up to the dimensions of the joint width between the soldered parts can cause the change of solder structure from ductile to quasi-ductile and later to quasi-brittle one, until the brittle fracture mode is attained.

Acknowledgements The work was supported by the Office of Government of Slovakia, project no. 09I03-03-V01-00047; by the Slovak Scientific Grant Agency under grant nos. VEGA 1/0389/22 and VEGA 2/0144/21; by the SRDA project APVV SK-UA-21-0076; by Ministry of Education and Science of Ukraine, projects nos. 0122U002643, 0122U001521; and by the Austrian Science Fund (FWF), project no. P 34894. The study was performed during the implementation of the project Building-up Centre for advanced materials application of the Slovak Academy of Sciences, ITMS project code 313021T081 supported by Research & Innovation Operational Programme funded by the ERDF.

Funding Open access funding provided by Austrian Science Fund (FWF).

Declarations

Conflict of interest The authors declare that they have no competing interests.

Open Access This article is licensed under a Creative Commons Attribution 4.0 International License, which permits use, sharing, adaptation, distribution and reproduction in any medium or format, as long as you give appropriate credit to the original author(s) and the source, provide a link to the Creative Commons licence, and indicate if changes were made. The images or other third party material in this article are included in the article's Creative Commons licence, unless indicated otherwise in a credit line to the material. If material is not included in the article's Creative Commons licence and your intended use is not permitted by statutory regulation or exceeds the permitted use, you will need to obtain permission directly from the copyright holder. To view a copy of this licence, visit http://creativecommons.org/licenses/by/4.0/.

References

Aspalter A, Cerny A, Göschl M, Podsednik M, Khatibi G, Yakymovych A, Plevachuk Yu (2020) Hybrid solder joints: morphology and shear strength of Sn–3.0Ag–0.5Cu solder joints by adding ceramic nanoparticles through flux doping. ApplNanosci 10:4943–4949. https://doi.org/10.1007/s13204-020-01398-8

Chen B, Wang H, Zou M, Hu X, Chen W, Jiang X (2022) Evolution of interfacial IMCs and mechanical properties of Sn–Ag–Cu solder joints with Cu-modified carbon nanotubes. J Mater Sci-Mater El 33:19160–19173. https://doi.org/10.1007/s10854-022-08753-1

Cheng F, Gao F, Nishikawa H, Takemoto T (2009) Interaction behavior between the additives and Sn in Sn–3.0Ag–0.5Cu-based solder alloys and the relevant joint solderability. J Alloys Compd 472:530–534. https://doi.org/10.1016/j.jallcom.2008.05.017

Cheng S, Huang CM, Pecht M (2017) A review of lead-free solders for electronics applications. Microelectron Reliab 75:77–95. https://doi.org/10.1016/j.microrel.2017.06.016

Fawzy A, Fayek SA, Sobhy M, Nassr E, Mousa MM, Saad G (2013) Effect of ZnO nanoparticles addition on thermal, microstructure and tensile properties of Sn–3.5 Ag–0.5 Cu (SAC355) solder alloy. J Mater Sci-Mater El 24:3210–3218. https://doi.org/10.1007/s10854-013-1230-2

Frear DR, Vianco PT (1994) Intermetallic growth and mechanical behavior of low and high melting temperature solder alloys. Metall Mater Trans A 25:1509–1523. https://doi.org/10.1007/BF02665483

Gain AK, Chan YC, Yung WKC (2011a) Microstructure, thermal analysis and hardness of a Sn–Ag–Cu–1 wt% nano-TiO2 composite solder on flexible ball grid array substrates. Microelectron Reliab 51:975–984. https://doi.org/10.1016/j.microrel.2011.01.006

Gain AK, Chan YC, Yung WKC (2011b) Effect of additions of ZrO_2 nano-particles on the microstructure and shear strength of Sn–Ag–Cu solder on Au/Ni metallized Cu pads. Microelectron Reliab 51:2306–2313. https://doi.org/10.1016/j.microrel.2011.03.042

Gain GAK, Fouzder T, Chan YC, Yung WKC (2011c) Microstructure, kinetic analysis and hardness of Sn–Ag–Cu–1 wt% nano-ZrO2 composite solder on OSP-Cu pads. J Alloys Compd 509:3319–3325. https://doi.org/10.1016/j.jallcom.2010.12.048

Han YD, Jing HY, Nai SML, Xu LY, Tan CM, Wei J (2012) Interfacial reaction and shear strength of Ni-coated carbon nanotubes reinforced Sn–Ag–Cu solder joints during thermal cycling. Intermetallics 31:72–78. https://doi.org/10.1016/j.intermet.2012.06.002

Haseeb ASMA, Arafat MM, Johan MR (2012) Stability of molybdenum nanoparticles in Sn–3.8Ag–0.7Cu solder during multiple reflow and their influence on interfacial intermetallic compounds. Mater Charact 64:27–35. https://doi.org/10.1016/j.matchar.2011.11.006

Hwang CW, Lee JG, Suganuma K, Mori H (2003) Interfacial microstructure between Sn-3Ag-xBi alloy and Cu substrate with or without electrolytic Ni plating. J Electron Mater 32:52–62. https://doi.org/10.1007/s11664-003-0237-5

Kartel M, Sementsov Yu, Mahno S, Trachevskiy V, Bo W (2016) Polymer Composites Filled with Multiwall Carbon Nanotubes. Univers J Mater Sci 4(2):23–31. https://www.hrpub.org/download/20160229/UJMS2-16205712.pdf

Kumar KM, Kripesh V, Tay AAO (2008) Single-wall carbon nanotube (SWCNT) functionalized Sn–Ag–Cu lead-free composite solders. J Alloys Compd 450:229–237. https://doi.org/10.1016/j.jallcom.2006.10.123

Kumar MP, Gergely G, Koncz-Horváth D, Gácsi Z (2020) Characterization of the interface between ceramics reinforcement and lead-free solder matrix. Surf Interfaces 20:100576. https://doi.org/10.1016/j.surfin.2020.100576

Kumar MP, Gergely G, Koncz-Horváth D, Gácsi Z (2021) Investigation of microstructure and wetting behavior of Sn–3.0Ag–0.5Cu (SAC305) lead-free solder with additions of 1.0 wt % SiC on copper substrate. Intermetallics 128:106991. https://doi.org/10.1016/j.intermet.2020.106991

Laurila T, Vuorinen V, Kivilahti JK (2005) Interfacial reactions between lead-free solders and common base materials. Mat Sci Eng R 49(1–2):1–60. https://doi.org/10.1016/j.mser.2005.03.001

Leong JC, Tsao LC, Fang CJ, Chu CP (2011) Effect of nano-TiO2 addition on the microstructure and bonding strengths of Sn3.5Ag0.5Cu composite solder BGA packages with immersion Sn surface finish. J Mater Sci-Mater El 22:1443–1449. https://doi.org/10.1007/s10854-011-0327-8

Li JF, Agyakwa PA, Johnson CM (2012) Effect of trace Al on growth rates of intermetallic compound layers between Sn-based solders and Cu substrate. J Alloys Compd 545:70–79. https://doi.org/10.1016/j.jallcom.2012.08.023

Li X, Yao Y (2017) Effect of cryogenic treatment on mechanical properties and microstructure of solder joint. In 18th International Conference on Electronic Packaging Technology (ICEPT)—Proceedings. Harbin, China 2017, pp 1327–1330. https://ieeexplore.ieee.org/document/8046683

Li ZH, Tang Y, Guo QW, Li GY (2019) Effects of CeO_2 nanoparticles addition on shear properties of low-silver Sn-0.3Ag-0.7Cu-xCeO_2 solder alloys. J Alloys Compd 789:150–162. https://doi.org/10.1016/j.jallcom.2019.03.013

Li Y, Yan X, Fu G, Wan B, Jiang M, Zhang W (2020) Failure Analysis of SAC305 Ball Grid Array SolderJoint at Extremely Cryogenic Temperature. Appl Sci 10:1951(1–16). https://www.mdpi.com/2076-3417/10/6/1951

Li M, Zhang L, Jiang N, Zhang L, Zhong S (2021) Materials modification of the lead-free solders incorporated with micro/nano-sized particles: a review. Mater Des 197:109224(2–34). https://doi.org/10.1016/j.matdes.2020.109224

Lupinacci A, Shapiro AA, Suh JO, Minor AM (2013) A study of solder alloy ductility for cryogenic applications. In 2013 IEEE International Symposium on Advanced Packaging Materials—Proceedings. Irvine, CA, USA, 2013, pp 82–88. https://ieeexplore.ieee.org/document/6510390

Marques VMF, Johnston C, Grant PS (2013) Nanomechanical characterization of Sn–Ag–Cu/Cu joints–Part 1: Young's modulus, hardness and deformation mechanisms as a function of temperature. Acta Mater 61:2460–2470. https://doi.org/10.1016/j.actamat.2013.01.019

Nai SML, Wei J, Gupta M (2008) Effect of carbon nanotubes on the shear strength and electrical resistivity of a lead-free solder. J Electron Mater 37(4):515–522. https://doi.org/10.1007/s11664-008-0379-6

Nai SML, Wei J, Gupta M (2009) Interfacial intermetallic growth and shear strength of lead-free composite solder joints. J Alloys Compd 473:100–106. https://doi.org/10.1016/j.jallcom.2008.05.070

Nieto-Marquez A, Romero R, Romero A, Valverde JL (2011) Carbon nanospheres- synthesis, physicochemical properties and applications. J Mater Chem 21:1664–1672. https://pubs.rsc.org/en/Content/ArticleLanding/2011/JM/C0JM01350A

Plevachuk Y, Tkach O, Švec P, Yakymovych A, Švec P, Orovcik L (2019) Nanocomposite solders: an influence of un-coated and Aucoated carbon nanotubes on morphology of Cu/Sn–3.0Ag–0.5Cu/Cu solder joints. In: 2019 IEEE 2nd Ukraine Conference on Electrical and Computer Engineering, UKRCON 2019 Proceedings. Lviv, Ukraine, 2019. pp 722–725. https://doi.org/10.1109/UKRCON.2019.8879891

Rud AD, Kuskova NI, Boguslavskii LZ, Kiryan IM, Petrichenko SV, Nazarova NS, Rodionova VN (2012) Electric Discharge Plasmochemical Synthesis of Carbon Nanomaterials. Nanomaterials: Application & Properties—Proceedings. 1(1):01NDLCN10(4P). https://nap.sumdu.edu.ua/index.php/nap/nap2012/paper/view/748/74

Rud AD, Polunkin IV KNE, Boguslavskii LZ, Vinnichenko DV, Kirian IM, Kolomys OF, Kuskova NI (2023) Structure of carbon nanospheres modifed with oxygencontaining groups and halogens. ApplNanosci. https://doi.org/10.1007/s13204-023-02817-2

Tan AT, Tan AW, Yusof F (2015) Influence of nanoparticle addition on the formation and growth of intermetallic compounds (IMCs) in Cu/Sn–Ag–Cu/Cu solder joint during different thermal conditions. Sci Technol Adv Mat 16:033505(18). https://doi.org/10.1088/1468-6996/16/3/033505

Tian R, Hang C, Tian Y, Zhao L (2018) Growth behavior of intermetallic compounds and early formation of cracks in Sn-3Ag-0.5Cu solder joints under extreme temperature thermal shock. Material Science and Engineering A 709:125–133. https://doi.org/10.1016/j.msea.2017.10.007

Tsao LC (2011a) Suppressing effect of 0.5 wt.% nano-TiO2 addition into Sn–3.5Ag–0.5Cu solder alloy on the intermetallic growth with Cu substrate during isothermal aging. J Alloys Compd 509:8441–8448. https://doi.org/10.1016/j.jallcom.2011.05.116

Tsao LC (2011b) Evolution of nano-Ag3Sn particle formation on Cu–Sn intermetallic compounds of Sn3.5Ag0.5Cu composite solder/Cu during soldering. J Alloys Compd 509:2326–2333. https://doi.org/10.1016/j.jallcom.2010.11.010

Wang Y, Zhao XC, Xie XC, Gu Y, Liu Y (2015) Effects of nano-SiO2 particles addition on the microstructure, wettability, joint shear force and the interfacial IMC growth of Sn3.0Ag0.5Cu solder. J Mater Sci-Mater El 26:9387–9395. https://doi.org/10.1007/s10854-015-3151-8

Wu CML, Yu DQ, Law CMT, Wang L (2004) Properties of lead-free solder alloys with rare earth element additions. Mater Sci Eng R 44:1–44. https://doi.org/10.1016/j.mser.2004.01.001

Wu M, Wang S, Sun W, Hong M, Chen Y, Ke L (2021) Fracture pattern evolution of SnAgCu−SnPb mixed solder joints at cryogenic temperature. Trans Nonferrous Met Soc China. 31:2762−2772. http://tnmsc.csu.edu.cn/down/2021/09_en/18-p2762.pdf

Wu YJ, Sees JA, Pouraghabagher C, Foster LA, Marshall JL, Jacobs EG, Pinizzoto RF (1993) The Formation and Growth of Intermetallics in composite solder. J Electron Mater 22:769–777. https://doi.org/10.1007/BF02817353

Yakymovych A, Plevachuk Yu, Švec P, Švec P, Janičkovič D, Šebo P, Beronská N, Roshanghias A, Ipser H (2016) Morphology and shear strength of lead-free solder joints with Sn3.0Ag0.5Cu solder paste reinforced with ceramic nanoparticles. J Electron Mater 45(12):6143–6149. https://doi.org/10.1007/s11664-016-4832-7

Yakymovych A, Plevachuk Yu, Švec P Sr, Janičkovič D, Šebo P, Beronská N, Nosko M, Orovcik L, Roshanghias A, Ipser H (2017a) Nanocomposite SAC solders: morphology, electrical and mechanical properties of Sn–3.8Ag–0.7Cu solders by adding Co nanoparticles. J Mater Sci-Mater El 28(15):10965–10973. https://doi.org/10.1007/s10854-017-6877-7

Yakymovych A, Plevachuk Yu, Sklyarchuk V, Sokoliuk B, Galya T, Ipser H (2017b) Microstructure and electro-physical properties of Sn-3.0Ag-0.5Cu nanocomposite solder reinforced with ni

nanoparticles in the melting-solidification temperature range. J Phase Equilib Diffus 38:217–222. https://doi.org/10.1007/s11669-017-0532-0
Yakymovych A Sr, Švec P, Orovcik L, Bajana O, Ipser H (2018) Nanocomposite SAC solders: the effect of adding Ni and Ni–Sn nanoparticles on morphology and mechanical properties of Sn–3.0Ag–0.5Cu solders. J Electron Mater 47(1):117–123. https://doi.org/https://doi.org/10.1007/s11664-017-5834-9
Yakymovych A, Slabon A, Švec PS, Plevachuk Yu, Orovcik L, Bajana O (2020) Nanocomposite SAC solders: the effect of adding CoPd nanoparticles on the morphology and the shear strength of the Sn–3.0Ag–0.5Cu/Cu solder joints. ApplNanosci 10:4603–4607. https://doi.org/10.1007/s13204-020-01325-x
Yakymovych A, Plevachuk Yu, Orovcik L, Švec P Sr (2022) Nanocomposite SAC Solders: the effect of heat treatment on the morphology of Sn-3.0Ag-0.5Cu/Cu solder joints reinforced with Ni and Ni-Sn Nanoparticles. ApplNanosci 12:977–982. https://doi.org/10.1007/s13204-021-01750-6

Publisher's Note Springer Nature remains neutral with regard to jurisdictional claims in published maps and institutional affiliations.